



ELSEVIER

Journal of Molecular Catalysis A: Chemical 163 (2000) 269–282

JOURNAL OF
MOLECULAR
CATALYSIS
A: CHEMICAL

www.elsevier.com/locate/molcata

Reaction network of pyridine hydrodenitrogenation over carbide and sulfide catalysts

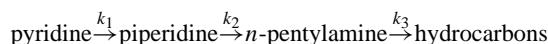
Viviane Schwartz, S. Ted Oyama*

Department of Chemical Engineering, Environmental Catalysis and Materials Laboratory,
Virginia Polytechnic Institute and State University, Blacksburg, VA 24061-0211, USA

Received 14 February 2000; accepted 18 April 2000

Abstract

A series of carbide and sulfide catalysts comprising NbMo₂C, Mo₂C, NbC and MoS₂/SiO₂ was used to study the pyridine hydrodenitrogenation (HDN) network below at high pressure (3.1 MPa) as a function of temperature.



All the catalysts showed the same trend in activities for the three molecules: the reactivity of *n*-pentylamine was high, while those of piperidine and pyridine were relatively low, especially at low temperatures. The carbide catalysts showed higher selectivity towards HDN products than the sulfide catalyst at the same conversion levels. The higher selectivity was related to the higher ratio ($r = k_2/k_1$) between the rate constants of the two consecutive reactions, hydrogenation of pyridine (k_1) and ring opening of piperidine (k_2). The order of activity of the carbides and sulfide differed considerably depending on the substrate. At the same temperature, the sulfide was more active for pyridine HDN when compared to the carbide catalysts, but it was much less active for quinoline HDN, suggesting that the HDN reaction mechanism depends greatly on the structure of the N-containing molecule. However, for the pyridine reaction network the similarity in product distribution suggested that the active surface of the carbides and sulfide was similar at reaction conditions. © 2000 Elsevier Science B.V. All rights reserved.

Keywords: Pyridine hydrodenitrogenation; Carbides; Sulfides; Selectivity; Rate constants

1. Introduction

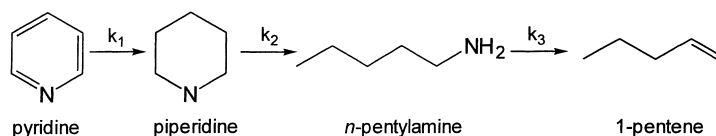
In the first companion paper [1], the mechanism of carbon–nitrogen bond cleavage for a series of aliphatic amines was investigated over two carbide catalysts and a reference sulfide catalyst. The results suggested that a β -elimination mechanism is the main reaction path for the C–N bond cleavage over all the catalysts. The objective of the present paper is to examine in detail

the reaction network leading to the formation of one of the aliphatic amines, *n*-pentylamine, namely hydrogenation of pyridine and hydrogenolysis of piperidine. Our approach is to study the principal reaction steps individually and thus to learn about their impact on the HDN reaction network.

It is well known that hydrogenation of the N-heterocyclic ring is required prior to the C–N bond cleavage in HDN reactions [2]. A difficulty arises from the fact that no single-limiting step was found in the literature [2–7]. That occurs because the reaction rates for both steps are of a similar order of

* Corresponding author. Fax: +1-540-231-5022.

E-mail address: oyama@vt.edu (S.T. Oyama).



Scheme 1. Reaction scheme for HDN of pyridine.

magnitude and are dependent on the structure of the N-containing compound and the reaction conditions. There is general agreement, however, that the two catalytic functions necessary for HDN, hydrogenation and C–N bond cleavage, are carried out at different catalytic sites [7–10]. Under industrial conditions, H₂S will always be present since sulfur compounds always accompany nitrogen compounds in petroleum feedstocks. The presence of H₂S has been studied by several groups and is reported to have a dual effect on the HDN catalytic activity: reduction of hydrogenation rates and promotion of C–N bond cleavage reactions [8].

For our work, pyridine HDN was chosen because only a few intermediates are formed and because many of the nitrogen compounds, which occur naturally in petroleum, are pyridine derivatives. The reaction scheme can be depicted for this case as a sequential series (Scheme 1).

Most of the studies reported deal with the kinetics of pyridine HDN on both sulfided and reduced Ni–Mo and Co–Mo supported on Al₂O₃ [11–14]. It was found that under most reaction conditions, the first step, hydrogenation of pyridine to piperidine, as well as the second step, formation of pentylamine from C–N bond cleavage of piperidine, are both similarly slow. In order to extend the work to carbide catalysts, knowledge of the conversion rates of pyridine and piperidine relative to *n*-pentylamine are necessary. In summary, the aim of this study is to investigate the pyridine HDN and the role of the intermediates, piperidine and *n*-pentylamine, over Mo₂C, NbC, and NbMo₂C, and to compare the results to MoS₂ supported on neutral SiO₂. The reactions are carried out in liquid-phase and high pressures to mimic the characteristic behavior of basic nitrogen compounds under industrial conditions. As will be reported, the behavior of the carbide and sulfide catalysts is remarkably similar, indicating that a common reaction sequence is operative during HDN on these materials. This substantiates the results

presented in the first companion paper [1] which showed that the mechanism of N-removal from amines, β-elimination, was the same on carbides and sulfides.

2. Experimental

2.1. Materials

Materials used for the preparation of the catalysts were: molybdenum(VI) oxide (MoO₃, 99.95%, Johnson Matthey), niobium(V) oxide (Nb₂O₅, 99.9%, Johnson Matthey), silica (SiO₂, Degussa) with surface area of 90 m² g⁻¹, and (NH₄)₆Mo₇O₂₄·4H₂O (Aldrich Chemical Co., A.C.S. reagent). The gases employed were He (Air Products, 99.999%), CH₄ (Air Products, UHP Grade), H₂ (Air Products, 99.999%), N₂ (Air Products, 99.999%), 0.5% (v/v) O₂/He (Air Products, 99.999%), 30% N₂/He (Air Products, 99.999%), CO (Air Products, 99.3%), 10% (v/v) H₂S/H₂ (Air Products, 99.999%). For the reactivity tests, the chemicals employed were: dibenzothiophene (Aldrich, 99.5%), quinoline (Aldrich, 99.9%), benzofuran (Aldrich, 99.9%), tetralin (Aldrich, 99.5%) and tetradecane (Jansen Chimica, 99%), pyridine (Aldrich, 99%), piperidine (Aldrich, 99%), *n*-pentylamine (Acros, 99%), dimethyl disulfide (Aldrich, 99%), octane (Acros, 99%). All chemicals were used as received. CH₄, H₂, N₂ and 30% N₂/He were passed through water purifiers (Alltech, model no. 8121) positioned in the line between the gas cylinders and the reactor, while He and CO were passed through a water/oxygen-removing purifier (Alltech, model no. 8121 and 4004).

2.2. Synthesis and characterization of catalysts

The synthesis of the bimetallic carbide involved two stages. First, the bimetallic oxide precursor was

prepared by the solid-state fusion of two monometallic oxides with a metal ratio (Mo/Nb) equal to 2.0. Second, the precursor material was carburized by temperature-programmed reaction using a reactive gas flow of 20% CH₄/H₂ up to a temperature of 1063 K. For the preparation of the monometallic Mo₂C and NbC, only the second step applied, with the corresponding single metal oxides being used for the carburization. Two 5.5 wt.% MoS₂/SiO₂ catalysts were used as the sulfide references. They were prepared in situ by flowing 100 μmol s⁻¹ (150 cm³ min⁻¹, NTP) of 10% H₂S/H₂ over 5 wt.% MoO₃/SiO₂ for 2 h at 673 K.

The catalysts were characterized by CO chemisorption (O₂ chemisorption for the sulfide catalysts), temperature programmed desorption (TPD) of ethylamine, N₂ physisorption, and X-ray diffraction (XRD). The values of CO and O₂ chemisorption were used for the calculation of turnover rates. TPD of ethylamine provided a means to count the number of Brønsted acid sites and served as another basis of comparison of catalytic activities. Surface areas were determined by N₂ physisorption, while XRD patterns were acquired using the powder method. The reactivity of all catalysts was tested for HDN of quinoline and HDS of dibenzothiophene in a three-phase, trickle-bed reactor. Details about the synthesis and characterization procedures are described in the first companion paper [1].

2.3. Pyridine/piperidine/pentylamine reactivity

The reactivity of the three amines (pyridine, piperidine and *n*-pentylamine) was determined separately in a trickle-bed reactor, employing liquid phase conditions at 3.1 MPa and various temperatures. Prior to the catalytic test, the carbides were activated in flowing H₂, while the Mo/SiO₂ catalyst was sulfided with a 10% H₂S/H₂ gas mixture. Importantly, the amount of catalysts employed in the tests was comparable. In the case of the carbides, the amount corresponded to 70 μmol of CO uptake, and in the case of the sulfide, it corresponded to 56 μmol of atomic oxygen uptake. The feed composition consisted of 2000 ppm of nitrogen (amine), 2000 ppm of octane (internal standard) and 3000 ppm of sulfur (dimethyl disulfide) in a tetradecane solvent. The H₂ flow rate was 110 μmol s⁻¹ (150 cm³/min, NTP) and the liquid feed was introduced at a rate of 5 cm³ h⁻¹. The testing

unit is described in detail in the companion paper [1]. Because of the low liquid rates and the good mixture provided by the hydrogen flow, the reactor operated as a CSTR.

Before each change in conditions and reagent, the reaction system was allowed to run for 60 h to be sure it had reached steady-state. Liquid samples were collected at regular intervals and the average of the steady-state values was used for the calculation of conversion and product distribution. Periodic recheck of catalytic activity at standard conditions after several experiments demonstrated that there was no deactivation. Again, as with the amines work [1], measurements were carried out for several months on each catalyst. The liquid samples were analyzed off-line by gas chromatography (Hewlett-Packard, 5890 Series II) using a fused silica capillary column (CPSIL-5CB) and a flame ionization detector. The reaction products were identified by GC-MS (VG Quattro, triple quadrupole, EI positive method) and the results of the identification were confirmed by the injection of standard compounds. Retention times of all possible reaction products were also obtained by injecting standards. Analysis of the gas-phase revealed the presence of the same light hydrocarbons found in the liquid-phase. Since only the analysis of the liquid phase was performed during the tests, vapor-liquid equilibrium curves [15] were used to obtain a correction factor for each of the C₅ hydrocarbons in order to take into account the products remaining in the gas-phase. The mass balance closed to 100% ± 10%.

3. Results

Conversions of pyridine, piperidine, and *n*-pentylamine were investigated as a function of temperature for the carbide catalysts (NbMo₂C, Mo₂C, and NbC) and the sulfide reference MoS₂/SiO₂ (Fig. 1). The results obtained for the monometallic NbC catalyst are not presented here and will not be discussed any further since it showed the same conversion levels obtained for a blank reactor. SiO₂ was used as a support for the sulfide catalyst due to its inert character and consequently small interaction with the sulfided phase [16]. The same conversion trend was found for all the catalysts. The reactivity of *n*-pentylamine was relatively high, while the conversion of piperidine

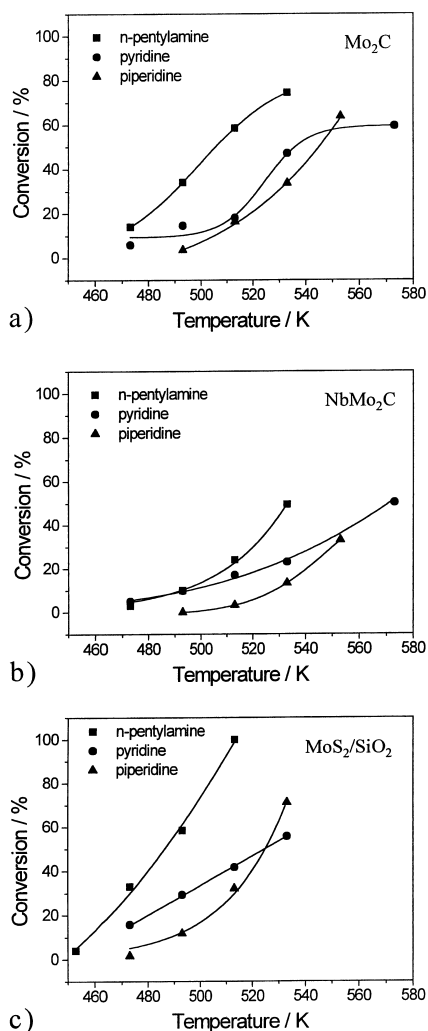


Fig. 1. Conversion of *n*-pentylamine, piperidine, and pyridine over: (a) Mo₂C; (b) NbMo₂C; (c) MoS₂/SiO₂.

was low, especially at low temperatures. As will be discussed later, the hydrogenation route of pyridine to piperidine is not limited by thermodynamic equilibrium at the experimental conditions employed in this study. Details about the characterization results for the catalysts used during this work can be found in the companion paper [1].

The effect of temperature on the product distributions of *n*-pentylamine, piperidine and pyridine for Mo₂C, NbMo₂C, and MoS₂/SiO₂, are shown respectively, in Figs. 2–4. Fig. 2 presents the results for the *n*-pentylamine reaction. The left panels show the

conversion and the overall product selectivity which consisted of C₅ hydrocarbons, condensation products, and sulfur products. The right panels show the details of the C₅ hydrocarbon distribution which consisted of pentane, found in the largest amounts, followed by 1-pentene, *trans*-2-pentene, and *cis*-2-pentene at higher conversions. In the case of NbMo₂C, the only C₅ product was pentane and a right panel is not shown (Fig. 2b). As discussed in the companion paper [1], these products are the result of a β-elimination type of mechanism. The condensation products were the N-containing compounds, dipentylamine and tripentylamine, which come from a disproportionation reaction. Tripentylamine was only present in small amounts at higher temperatures over the carbide catalysts. The condensation products are easily formed and are the main product in the low temperature range. They are also reported to be more reactive for C–N bond cleavage than is the primary amine [4]. In the case of *n*-pentylamine, the sulfur product was pentanethiol, formed by a substitution mechanism between the pentylamine (substrate) and hydrogen sulfide (nucleophile). Due to its high reactivity towards C–S bond cleavage, only small amounts of pentanethiol were found among the products. In comparing the three catalysts, it can be seen that Mo₂C (Fig. 2a) and MoS₂/SiO₂ (Fig. 2c) have the highest activities, and NbMo₂C (Fig. 2b) has the lowest.

Fig. 3 shows the results for the piperidine reaction. Again, the left panels show the conversion and overall selectivity, while the right panels show the C₅ product distribution. Pentylamine was never found among the products, while substantial amounts of condensation compounds were observed at low temperatures. In the case of the piperidine reaction, the condensation products were *N*-pentylpiperidine and in very low concentrations, *N*-butylpiperidine. The absence of *n*-pentylamine indicates that, at low temperatures, the most important consecutive reaction is not the formation of pentylamine by the opening of the piperidine ring, but the disproportionation of a piperidine molecule and *n*-pentylamine into ammonia and *N*-pentylpiperidine (Scheme 2). The sulfur products identified during this reaction were: tetrahydro-2H-thiopyran and small amounts of tetrahydro-2-methyl-thiophene. A reaction pathway is suggested for the formation of these molecules in the presence of hydrogen sulfide (Scheme 3) [17].

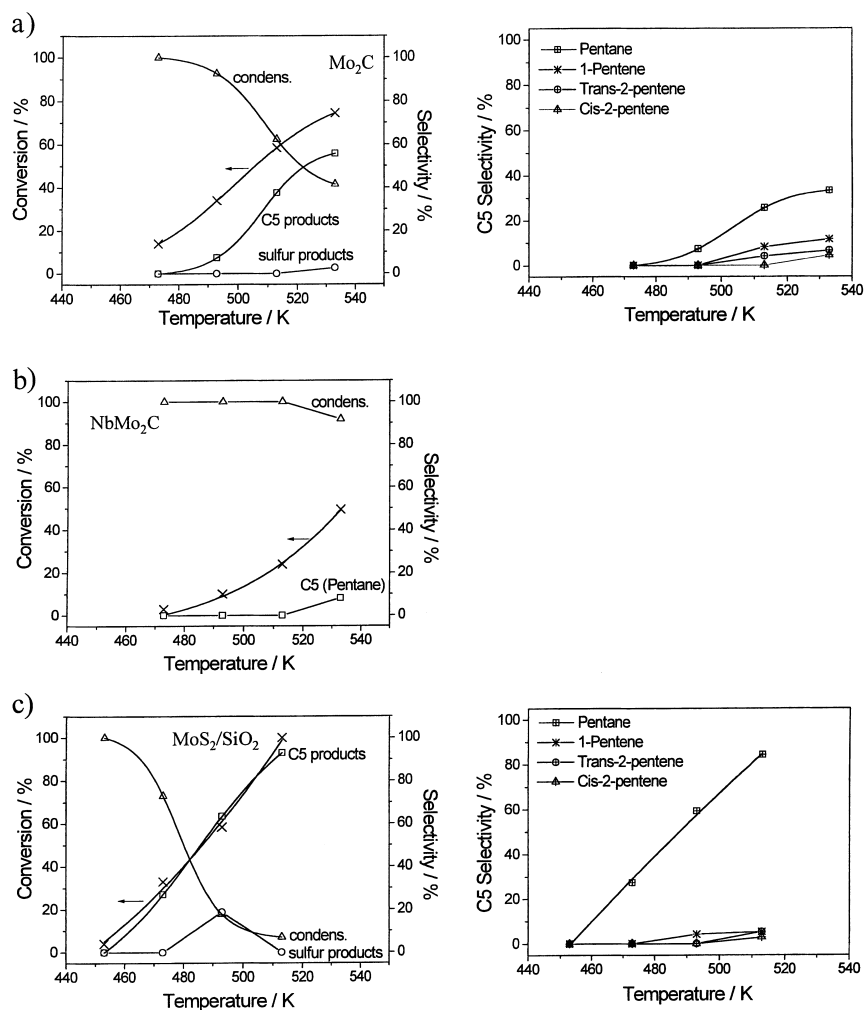


Fig. 2. Conversion and product distribution for the *n*-pentylamine reaction over: (a) Mo₂C; (b) NbMo₂C; (c) MoS₂/SiO₂.

In this scheme, the piperidine ring is opened as a result of C–N bond scission. Part of this compound undergoes a nucleophilic substitution reaction with hydrogen sulfide to give 4-pentene-1-thiol. The latter then cyclizes to tetrahydro-2H-thiopyran and tetrahydro-2-methyl-thiophene. The C₅ hydrocarbons found were the same as the ones found in the HDN of *n*-pentylamine with a similar product distribution. No pyridine was found among the products since the dehydrogenation reaction of piperidine is not thermodynamically favored at the reaction conditions used during this study. Among the C₅ hydrocarbon products, for all catalysts, the main product was pentane,

while smaller amounts of pentenes were obtained at higher conversions.

Fig. 4 shows the results for the pyridine reaction. Once again, the left panels report conversion and overall selectivity, while the right panels show the C₅ product distribution. The overall distribution is in agreement with that obtained in the piperidine reaction. At low conversions the main species observed was piperidine, the expected product from the first hydrogenation step, and a small amount of *N*-pentylpiperidine. As conversion increased C₅ hydrocarbons began to be produced, with pentane again being the most favored product.

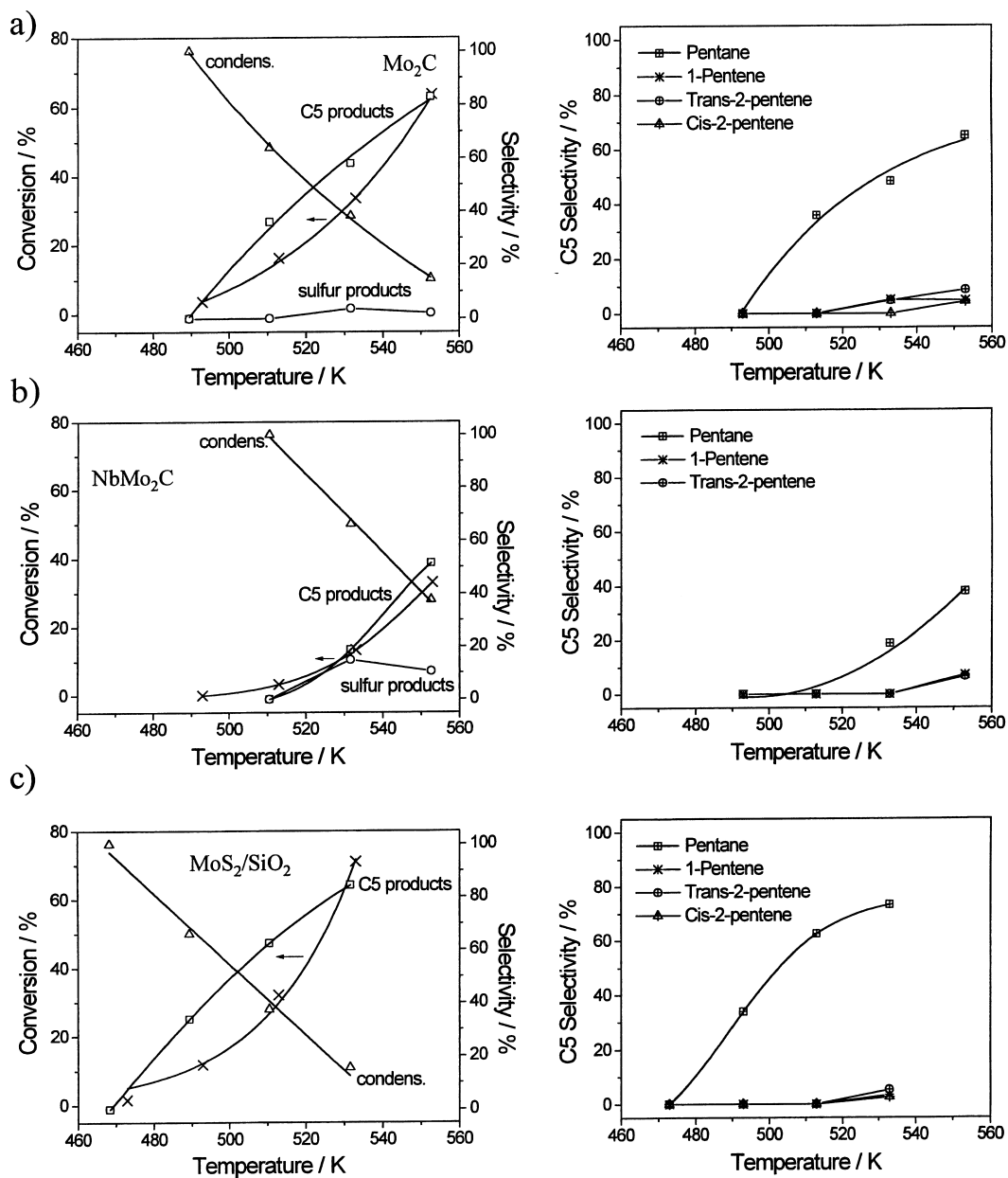


Fig. 3. Conversion and product distribution for the piperidine reaction over: (a) Mo_2C ; (b) NbMo_2C ; (c) $\text{MoS}_2/\text{SiO}_2$.

Analysis of the product distribution for piperidine and pyridine over the three catalysts at the same conversion levels are presented in Figs. 5 and 6. *n*-Pentylamine is not analyzed further since the deamination of the primary amine was found to be fast (Fig. 1) compared to the denitrogenation of the heterocyclic

nitrogen compounds. $\text{MoS}_2/\text{SiO}_2$ showed a slightly higher amount of denitrogenated products compared to the carbide catalysts for the piperidine reaction (Fig. 5). However, the carbides presented a considerable superiority regarding the concentration of HDN products when pyridine was used as reagent (Fig. 6).

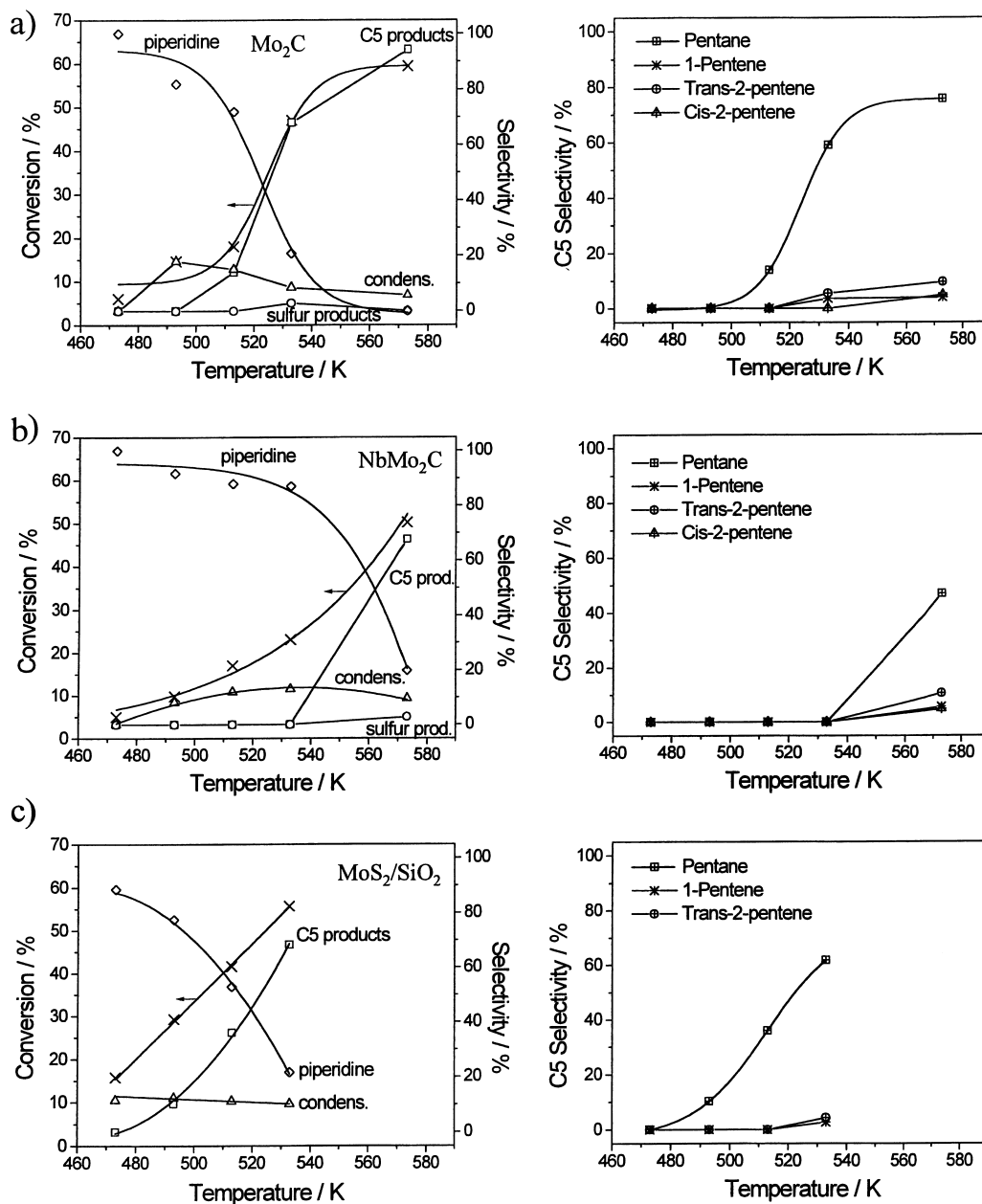


Fig. 4. Conversion and product distribution for the piperidine reaction over: (a) Mo_2C ; (b) NbMo_2C ; (c) $\text{MoS}_2/\text{SiO}_2$.

4. Discussion

Comparing the values of conversion of *n*-pentylamine (Fig. 1) with the two heterocyclic molecules, piperidine and pyridine, it is clear from the low tem-

perature of reaction that the aliphatic amine has a very high reactivity, regardless of the catalyst used. Further evidence of its high reactivity is finding that *n*-pentylamine is never formed as an intermediate product for the reactions of piperidine (Fig. 3) and

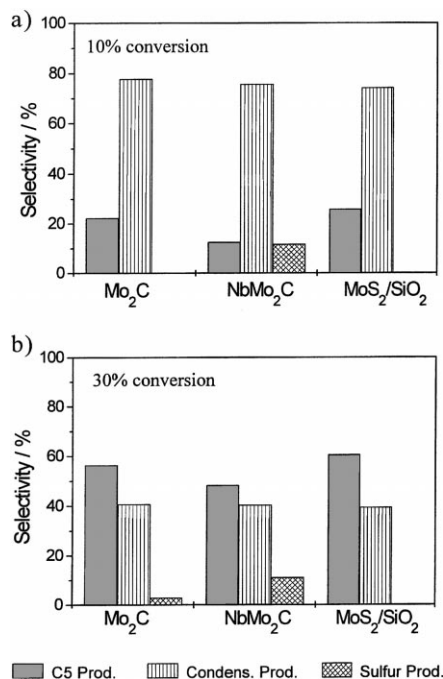


Fig. 5. Piperidine product distribution at constant conversion levels: (a) 10% conversion; (b) 30% conversion.

dine was the reagent. Also in the case of the pyridine reaction, it was found that hydrocarbons were formed at higher temperatures as piperidine disappeared from the products, indicating that ring opening preceded hydrocarbon formation.

Although the sulfide catalyst presented consistently higher conversions than the carbides at the same temperature, the latter had a superior selectivity towards HDN products at the same conversion levels (Fig. 6). The superiority is more evident at higher conversions. For example, at conversions of 40%, piperidine is still the major product over the sulfide catalyst, while Mo_2C already shows high yields of hydrocarbons. These results indicate that the ratio of rate constants ($r = k_2/k_1$) of the second step (hydrogenolysis of piperidine) to the first step (hydrogenation of pyridine) is smaller for the sulfide catalyst compared to the carbides. In order to obtain a better understanding of this situation, the relative rates are quantified below. Taking the simplified reaction network illustrated in Scheme 1, it is assumed that both steps are first-order and irreversible. This is reasonable considering that

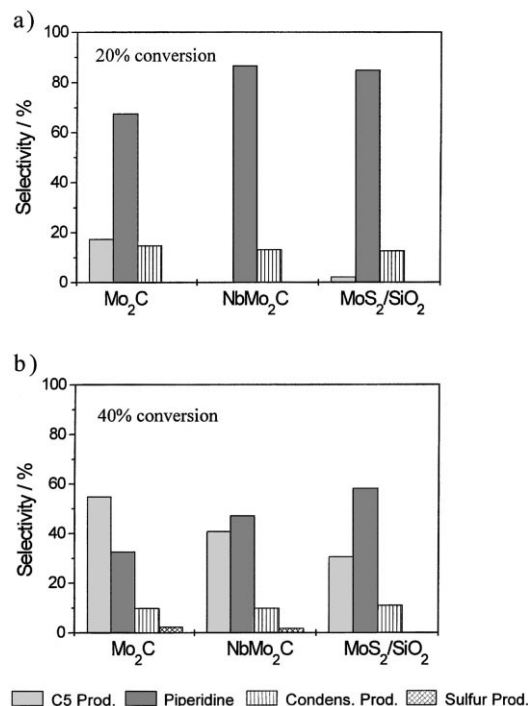


Fig. 6. Pyridine product distribution at constant conversion levels: (a) 20% conversion; (b) 40% conversion.

most studies [4,11,13] of the pyridine–piperidine reaction on sulfide catalysts can be fit to a first-order kinetic model and that the hydrogenation of pyridine is practically irreversible at our given reaction conditions. In this case, the rate of consumption of pyridine and the rate of formation of the intermediate, piperidine, would be represented as follow:

$$-v_{\text{PYR}} = k_1(\text{PYR}) \quad (2)$$

$$v_{\text{PIP}} = k_1(\text{PYR}) - k_2(\text{PIP}) \quad (3)$$

Since $-v_{\text{PYR}}$ represents the rate of formation of all products, the selectivity (S) for the piperidine intermediate can be defined as:

$$S = \frac{v_{\text{PIP}}}{-v_{\text{PYR}}} = 1 - \frac{k_2(\text{PIP})}{k_1(\text{PYR})} \quad (4)$$

The ratio, r , between the two rate constants, k_2 and k_1 , is obtained by rearranging the above expression:

$$r = \frac{k_2}{k_1} = (1 - S) \left(\frac{\text{PYR}}{\text{PIP}} \right) \quad (5)$$

Table 1
Pyridine HDN results for Mo₂C, NbMo₂C, and MoS₂/SiO₂^a

	<i>T</i> (K)	<i>X</i> (%)	<i>S</i> (%)	(PYR)/(PIP)	<i>r</i> = <i>k</i> ₂ / <i>k</i> ₁
Mo ₂ C	489	10.0	91.5	9.84	0.836
	504	12.8	83.6	8.20	1.345
	514	20.0	66.0	6.10	2.073
	518	25.0	57.6	5.20	2.206
	522	30.0	47.7	4.90	2.562
	528	40.0	32.8	4.60	3.091
	532	45.0	24.0	5.10	3.875
	536	50.0	16.4	6.10	5.098
NbMo ₂ C	506	13.2	93.2	7.06	0.480
	533	23.0	84.8	3.95	0.601
	542	27.3	78.7	3.38	0.720
	550	32.5	69.5	2.99	0.912
	558	38.2	57.1	2.83	1.214
	563	42.4	47.2	2.88	1.521
	569	47.8	33.1	3.30	2.208
	MoS ₂ /SiO ₂	480	20.0	85.0	4.71
487		25.0	80.0	3.75	0.750
495		30.0	74.7	3.13	0.792
503		35.0	66.6	2.79	0.932
510		40.0	58.0	2.59	1.088
517		45.0	48.7	2.51	1.287
525		50.0	36.4	2.75	1.750

^a *X*: conversion of pyridine and *S*: selectivity of piperidine. Values were interpolated from smoothed out conversion and selectivity curves in Figs. 2–4.

Values of selectivity and conversion were obtained for each catalyst for various temperatures in the range used during the study of the pyridine reaction (Fig. 4) and are summarized in Table 1. In order to obtain more points at lower temperatures and to smooth the fits, data were extrapolated from Fig. 4. The ratio of (PYR)/(PIP) is calculated from the values of conversion (*X*) and selectivity, since

$$S = \frac{(\text{PIP})}{(\text{PYR})_0 - (\text{PYR})} \quad \text{and}$$

$$X = \frac{(\text{PYR})_0 - (\text{PYR})}{(\text{PYR})_0},$$

which gives:

$$\frac{(\text{PYR})}{(\text{PIP})} = \frac{(1 - X)}{SX} \quad (6)$$

Table 1 also shows the calculated values for *r* obtained for each catalyst. It can be observed that the ratio, *r*, for the Mo₂C catalyst, which presents better selectivity for hydrocarbons products, is consistently higher than the

values obtained for the sulfide catalyst, as expected. In all cases, the ratio increases with temperature.

The difference in activation energies between the two steps of reaction can be related to the ratio, *r*, through the Arrhenius equation, as shown below:

$$r = \frac{A_2}{A_1} \exp \left[-\frac{E_2 - E_1}{RT} \right] \quad (7)$$

here *A*₁ and *A*₂ are the preexponential factors.

A plot of ln(*r*) versus 1/*T* is given for all the catalysts (Fig. 7) and the difference in activation energies between the first two steps of the pyridine HDN

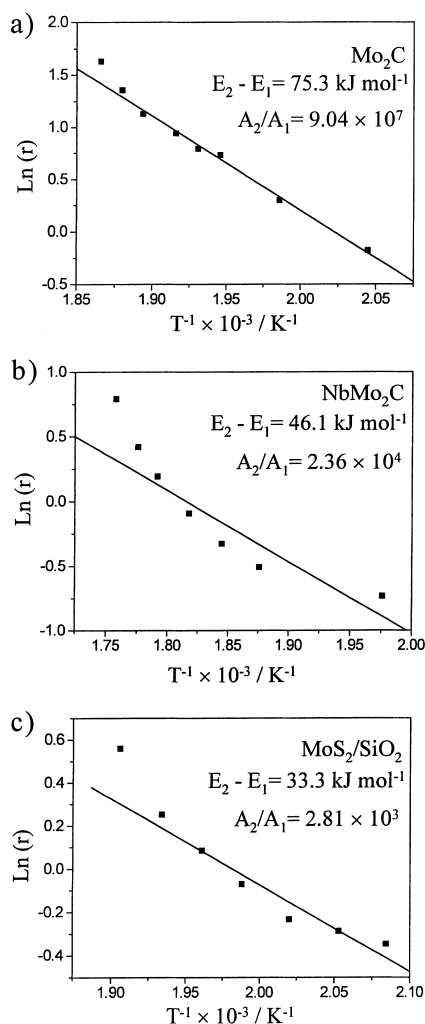
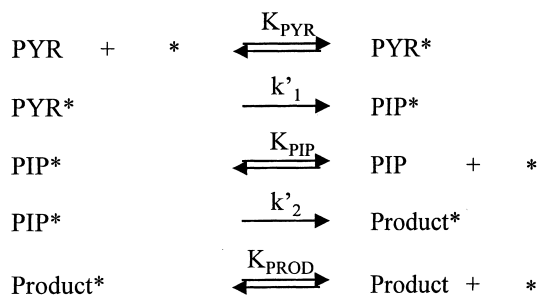


Fig. 7. ln(*r*) vs. 1/*T* plots for: (a) Mo₂C; (b) NbMo₂C; (c) MoS₂/SiO₂.



Scheme 4. Rake mechanism for the reaction network.

reaction is obtained from the slope of the plots. The points at high temperatures were not considered for the linear fit. In the case of the sulfide catalyst, the rupture of the heterocyclic ring requires 33.2 kJ mol^{-1} more than the hydrogenation of pyridine, while in the other extreme, for Mo_2C , the difference rises to 75.3 kJ mol^{-1} . The larger difference in activation energy combined with higher ratio of preexponential factor (A_2/A_1) is responsible for higher selectivities for hydrocarbon products at high temperatures and conversion. The bimetallic presented an intermediate value for the difference of activation energies between the second and first step equal to 46.1 kJ mol^{-1} . Selectivity for HDN products was also intermediate at higher temperatures as can be observed in Fig. 6.

Although instructive, this simplified analysis is not a rigorous representation of the actual catalytic reaction mechanism for pyridine HDN. A more detailed mechanism should describe the adsorption of the reagents on the catalyst surface and the surface reaction. Again, only the slow and equilibrated steps were taken into account during the development of the following and more detailed reaction scheme (Scheme 4). The scheme does not show the adsorption of hydrogen. The literature [8–10] indicates that hydrogen and the nitrogen-bases are adsorbed on different catalytic sites and at the high H_2 partial pressures used in these studies the hydrogen sites are likely to be saturated. The network shown involves the so-called rake mechanism (Scheme 4) [19]:

According to Scheme 4, at steady-state, the rates of the two unequilibrated steps, (v'_1 and v'_2) should be equal:

$$v'_1 = k'_1(\text{Pyr}^*) \quad (8)$$

$$v'_2 = k'_2(\text{PIP}^*) \quad (9)$$

From these equations, (Eqs. (8) and (9)), and the equilibrium expressions for (Pyr^*) and (PIP^*), we obtain a relation involving the hydrogenation of pyridine and the piperidine ring-opening steps:

$$\frac{k'_2}{k'_1} = \frac{K'_{\text{PRY}}(\text{Pyr})}{K'_{\text{PIP}}(\text{PIP})} \quad (10)$$

In this analysis, the ratio of rate constants, k'_2/k'_1 , involves contributions from the equilibrium constants of adsorption of pyridine and piperidine. We are unable to get these constants from the limited data available, but it can be seen that the value of k'_2/k'_1 is different from that of r , obtained by the simple analysis. Rearranging Eq. (10), we define a new r' :

$$r' = \frac{k'_2 K'_{\text{PIP}}}{k'_1 K'_{\text{PYR}}} = \frac{(\text{Pyr})}{(\text{PIP})} \quad (11)$$

For each temperature and conversion, a new value for the ratio, r' , between the rate of the ring-opening and hydrogenation step was obtained based on the ratio of concentrations of pyridine and piperidine, which are given on Table 1. The values of r' for the Mo_2C catalyst, which presents better selectivity for hydrocarbon products, is consistently higher than the values obtained for the sulfide catalyst. From Eq. (11), a new Arrhenius expression (Eq. (12)) is derived:

$$\begin{aligned}
 r' = & \frac{A'_2 A_{\text{PIP}}}{A'_1 A_{\text{PYR}}} \\
 & \times \exp \left[- \frac{[(E'_2 - \Delta H'_{\text{PIP}}) - (E'_1 - \Delta H'_{\text{PYR}})]}{RT} \right]
 \end{aligned} \quad (12)$$

For each of the three catalysts, a plot of $\ln(r')$ versus $1/T$ was produced (Fig. 8). The linear regression was again obtained after excluding the high temperature points. Based on the Arrhenius expression (Eq. (12)), the slope of the plots is related to the activation energies and the change in enthalpies for the adsorption steps. The overall energy changes are defined on the energy diagrams sketched on Fig. 9. In this case, the Arrhenius plots produced a positive slope for the low temperature points, consequently the difference $(E'_2 - \Delta H'_{\text{PIP}}) - (E'_1 - \Delta H'_{\text{PYR}})$, which includes the heats of adsorption of pyridine and piperidine, gives a

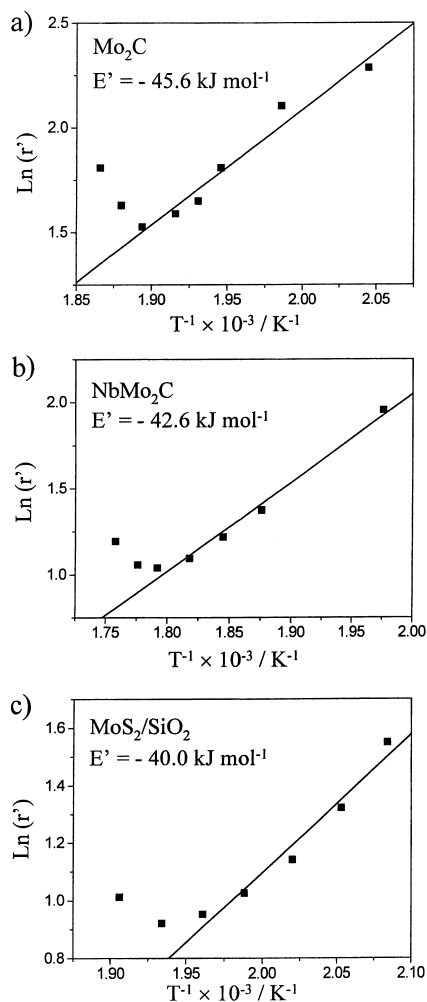


Fig. 8. $\ln(r')$ vs. $1/T$ plots for: (a) Mo_2C ; (b) $NbMo_2C$; (c) MoS_2/SiO_2 .

negative value. For the sulfide, the difference is equal to $-40.0 \text{ kJ mol}^{-1}$, while for Mo_2C is $-45.6 \text{ kJ mol}^{-1}$. The bimetallic presented again an intermediate value equal to $-42.6 \text{ kJ mol}^{-1}$. The similarity in the values for all catalysts can be rationalized if there is a linear free energy relationship between E' and $\Delta H'$ for the adsorption of pyridine and piperidine, and if the difference in the heats of adsorption are similar. This similarity was an unexpected and an a priori unlikely result, but it suggests that the mechanism on the three catalysts are likewise similar.

An overall comparison between the carbide catalysts and the sulfide reference presents a very

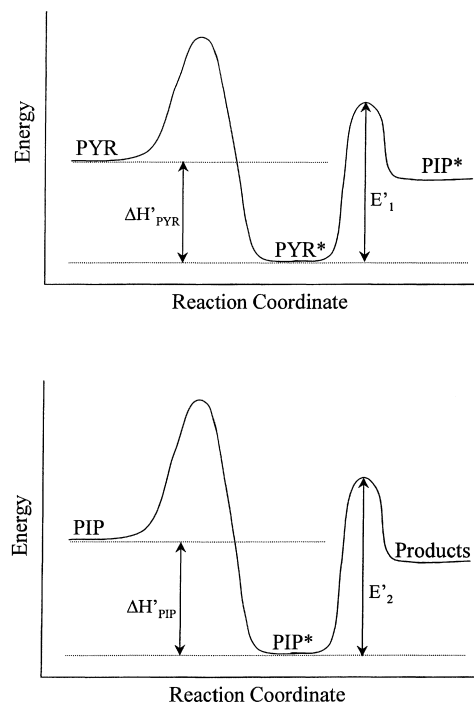


Fig. 9. Energy diagram sketch.

interesting aspect. The sulfide catalyst showed higher activity than the bimetallic carbide for all the probe molecules tested on this study, which were: *n*-pentylamine, piperidine and pyridine (Fig. 1). This is true whether the CO and O_2 uptakes or the number of Brønsted-acid sites were used for calculation of turnover rates [1]. On the other hand, the situation is completely reversed when the catalysts were compared for the simultaneous HDN of quinoline and HDS of dibenzothiophene. As described in our previous companion paper [1], for this catalytic test, MoS_2/SiO_2 presented small HDN (10%) and HDS (26%) conversions, compared to the results for $NbMo_2C$, which had high HDN (57%) and HDS (59%) conversions. Those results suggest that comparison of HDN activities have to be strictly related to the nature and structure of the probe molecules. For example, some studies in the literature [20,21] analyze the effect of alkyl substituents on the HDN of pyridine. The compounds derived from pyridine presented a large range of activity change [20]. In fact, the presence of substituents slows down both hydrogenation and hydrogenolysis [21]. If quinoline

is viewed as a benzo-substituted pyridine, the attachment of a benzene ring should have an even stronger influence than the alkyl substituents on the reactivity of pyridine. Another important aspect that differentiates the two molecules, pyridine and quinoline, is that the rate-limiting step of quinoline HDN is supposed to be the hydrogenation of the benzenic ring [7]. This fact makes difficult any comparison with the HDN of pyridine, which does not involve such a reaction.

The nature of the active sites is another point that should be addressed in this discussion. Studies [10,22,23] using sulfide catalysts for the HDN reaction associate two types of catalytic sites to the two different functions, hydrogenation and C–N bond cleavage. The sites for hydrogenation are thought to be related to sulphur anion vacancies while the sites active for the cleavage of the C–N bond seem to be acidic. In our previous studies [1] we have identified nucleophilic sulfide and electrophilic Brønsted acid sites as required for C–N bond cleavage on both carbides and sulfide. Therefore, different cases should be considered depending on the distance between the acidic and the hydrogenation sites. When they are adjacent, they form an entity able to catalyze the hydrogenation reactions as well as the C–N bond cleavage. The difference of the structure between the two molecules, pyridine and quinoline, together with the surface distribution of active sites on a given catalyst, might explain the large range of activities found for these two molecules with the same catalyst.

5. Conclusions

In this study, we investigated the pyridine HDN and the role of the intermediates, piperidine and *n*-pentylamine, over NbMo₂C, Mo₂C, NbC and MoS₂/SiO₂. The reactions were carried out in liquid phase and the N-containing molecules were studied separately. The products identified from the pyridine, piperidine and *n*-pentylamine reactions were the same for the carbides, as well as the sulfide catalyst, indicating that the reaction pathway was the same on all catalysts. Among the hydrocarbons products, 1-pentene was the most abundant olefin providing evidence for the contribution of a β -elimination type of mechanism. Comparison of the activities of the three molecules showed the same trend for all the catalysts.

The *n*-pentylamine reaction is very fast when compared to the hydrogenation of pyridine and the C–N bond cleavage of piperidine, as shown by the absence of *n*-pentylamine among the products of reaction.

The carbide catalysts showed higher selectivity towards HDN products than the sulfide catalyst at the same conversion levels. A first-order kinetic model gave a simple explanation for the results. The higher selectivity was related to the ratio between the rate constants of the two consecutive reactions: hydrogenation of pyridine and ring opening of piperidine. The higher the ratio, the higher the selectivity for hydrocarbons at high temperatures and conversions. Although the bimetallic carbide presented better selectivity at high conversions than the sulfide, the latter was more active when comparison was based on the same temperatures. The higher activity of the sulfide for the pyridine HDN compared to the small quinoline HDN activity allows us to conclude that the HDN reaction mechanism depends greatly on the structure of the N-containing molecule and the surface site distribution.

Acknowledgements

This paper was written with the support from the US Department of Energy, Office of Basic Energy Sciences, Grant No DE-FG02-963414669. V. Schwartz is grateful to CAPES (Brazil) for the scholarship received during the development of this work.

References

- [1] V. Schwartz, V.T. da Silva, S.T. Oyama, J. Mol. Catal. 163 (2000).
- [2] H. Topsøe, B.S. Clausen, F.E. Massoth, Hydrotreating Catalysts, Science and Technology, Springer, New York, 1991, p. 133.
- [3] T.C. Ho, Catal. Rev.-Sci. Eng. 301 (1) (1988) 117.
- [4] H. Shulz, M. Schon, N.M. Rahman, in: L. Cerveny (Ed.), Studies in Surface Science and Catalysis, Vol. 127, Elsevier, Amsterdam, 1986 (Chapter 6).
- [5] C.N. Satterfield, J.F. Cochetto, Ind. Eng. Chem. Proc. Des. Dev. 20 (1981) 53.
- [6] M. Cattenot, J.-L. Portefaix, J. Afonso, M. Breyse, M. Lacroix, G. Perot, J. Catal. 173 (1998) 366.
- [7] G. Perot, Catal. Today 10 (1991) 447.
- [8] J.K. Minderhoud, J.A.R. Van Veen, Fuel Proc. Tech. 35 (1993) 87.

- [9] R.T. Hanlon, *Energy Fuels* 1 (1987) 424.
- [10] S.H. Yang, C.N. Satterfield, *J. Catal.* 81 (1983) 168.
- [11] H.G. McIlvried, *Ind. Eng. Chem. Proc. Des. Dev.* 10 (1) (1971) 125.
- [12] J. Sonnemans, P. Mars, *J. Catal.* 31 (1973) 209.
- [13] C.D. Ajaka, R.S. Mann, *Ind. J. Tech.* 31 (1993) 131.
- [14] A. Calafat, J. Laine, A. Lopez-Agudo, *Catal. Lett.* 40 (1996) 229.
- [15] S.T. Hadden, H.G. Grayson, *Hydroc. Proc. Petrol. Refin.* 40 (1961) 207.
- [16] M. Breysse, J.L. Portefaix, M. Vrinat, *Catal. Today* 10 (1991) 489.
- [17] M. Cerny, *Coll. Czech. Chem. Commun.* 47 (1982) 928.
- [18] W.V. Steele, R.D. Chirico, Topical Report for the US Department of Energy, IIT Research Institute, Bartlesville, Oklahoma, 1992.
- [19] M. Boudart, G. Djéga-Mariadassou, *Kinetics of Heterogeneous Catalytic Reactions*, 1st Edition, Princeton University Press, New jersey, 1984.
- [20] K.E. Cox, L. Berg, *Chem. Eng. Prog.* 56 (1962) 54.
- [21] M. Cerny, *Coll. Czech. Chem. Commun.* 44 (1979) 85.
- [22] S.H. Yang, C.N. Satterfield, *Ind. Eng. Chem. Proc. Des. Dev.* 23 (1984) 20.
- [23] M. Callant, K.A. Holder, P. Grange, B. Delmon, *Bull. Soc. Chim. Belg.* 104 (4) (1995) 245.